# Enhanced Fructose Oxidase Activity in a Galactose Oxidase Variant

Sarah E. Deacon,[a] Khaled Mahmoud,[a] R. Kate Spooner,[a, b] Susan J. Firbank,[a, c] Peter F. Knowles,[a] Simon E. V. Phillips,[a] and Michael J. McPherson*[a]

*Galactose oxidase (GO; EC 1.1.3.9) catalyses the oxidation of a wide range of primary alcohols including mono-, oligo- and polysaccharides. High-resolution structures have been determined for GO, but no structural information is available for the enzyme with bound substrate or inhibitor. Previously, computer-aided docking experiments have been used to develop a plausible model for interactions between GO and the* D*-galactose substrate. Residues implicated in such interactions include Arg330, Gln406, Phe464, Phe194 and Trp290. In the present study we describe an improved expression system for recombinant GO in the methylotrophic yeast* Pichia pastoris*. We use this system to express variant proteins mutated at Arg330 and Phe464 to explore the substrate binding model. We also demonstrate that the Arg330 variants display greater fructose oxidase activity than does wild-type GO.*

## Introduction

Galactose oxidase (GO; EC 1.1.3.9) is secreted by *Fusarium graminearum*[1,2] (J. Pallas and M.J.M., unpublished data) and the heterologous expression host *Aspergillus nidulans*.[3] GO is a monomeric copper-containing oxidase that operates by a radical mechanism and catalyses the oxidation of a wide range of primary alcohols, including D-galactose (Figure 1 A), with production of the corresponding aldehyde. Reoxidation of the enzyme is achieved by reduction of dioxygen to hydrogen peroxide. GO is a member of the growing class of enzymes that contain a cofactor derived from active-site amino acids. In the case of GO the cofactor involves a thioether bridge between Cys228 and Tyr272 which contributes to the redox and stability properties of the radical at Tyr272. Interestingly, the thioether bridge is formed by autocatalytic events involving the copper centre.[4,5] Detailed spectroscopic studies,[6–11] X-ray crystallography[12,13] and study of site-directed mutations[3,14–16] have led to a reasonable understanding of the catalytic mechanism of GO.

To date, no crystallographic information on substrate or substrate-analogue binding to GO has been obtained. This may be due to packing of GO in the crystal lattice restricting access of monosaccharide substrates to the active site[13] or to inefficient substrate binding in the crystal as indicated by the high Michaelis constant, $K_M$, value (70–100 mM for D-galactose). By using the crystallographic structure of GO, a substrate binding model has been proposed,[12,13] which is consistent with published data on the catalytic mechanism and the known substrate specificity of the enzyme. A small depression suggestive of a possible substrate binding pocket was found on the sur-

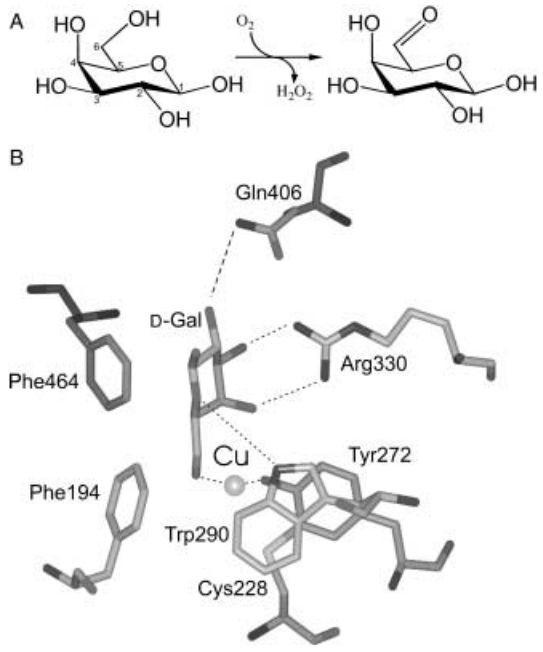


***Figure 1.*** *Galactose oxidase active site. A) Oxidation reaction of* D*-galactose to* D*-galactohexadialdose catalysed by GO. B) Model of* D*-galactose in the active site showing the proposed hydrogen-bond interactions.[17] The residues Arg330 and Phe464 are investigated in this study.*

[a] *S. E. Deacon, Dr. K. Mahmoud, Dr. R. K. Spooner, Dr. S. J. Firbank, Prof. Dr. P. F. Knowles, Prof. Dr. S. E. V. Phillips, Prof. Dr. M. J. McPherson*
*Astbury Centre for Structural Molecular Biology*
*School of Biochemistry and Molecular Biology*
*University of Leeds, Leeds, LS2 9JT (UK)*
*Fax: (+44) 113-233-3144*
*E-mail: m.j.mcpherson@leeds.ac.uk*

[b] *Dr. R. K. Spooner*
*Current address:*
*ProImmune Ltd., Oxford Biobusiness Centre*
*Littlemore Park, Oxford, OX4 4SS (UK)*

[c] *Dr. S. J. Firbank*
*Current address:*
*Institute of Biochemistry, University of Zürich*
*8057 Zürich (Switzerland)*

  DOI: 10.1002/cbic.200300810 

face of the enzyme at the copper site in domain 2. The residues around the pocket showed structural complementarity to the D-galactose "chair" conformation (Figure 1B). This substrate binding model, which has been refined by further modelling studies,[17] has the O(6) atom of D-galactose directly coordinated to the copper and locates the hydroxy groups on C(4) and C(3) of the substrate to within hydrogen-bond distance of the guanidinium side chain of Arg330. Gln406 may form a hydrogen bond with the O(2) atom and the nitrogen of the indole ring of Trp290 is suggested to form a hydrogen bond with the O(5) atom of D-galactose. The residues Phe194 and Phe464 provide a hydrophobic surface that may make hydrophobic interactions with the substrate.[13]

This model also explains the substrate specificity of the enzyme. D-Glucose, for example, is not a substrate and differs from D-galactose only in the orientation of the C(4) hydroxy group, which prevents an interaction with Arg330 and causes a steric clash with the side chain of Tyr495. This observation of steric hindrance may also explain the results of a study in which several 4-deoxy substitutents of D-galactose displayed differences in their ability to act as efficient substrates.[18] Wild-type GO is reported to display no activity against D-glucose or D-fructose.[19] Recently, Sun et al.[20] have reported site-directed mutagenesis experiments that have resulted in the acquisition of a low level of glucose oxidase activity within a GO variant containing three amino acid substitutions, R330K, W290F and Q406T. We are interested in developing altered versions of GO that display enhanced activity against D-fructose.

We have previously described a heterologous expression system for GO, based on *A. nidulans*,[3] which uses the maltose-inducible *A. awamori* glucoamylase promoter. While this system yields around 50 mg $L^{-1}$ of GO, the transformation frequency is low and generation of stable transformed lines is time-consuming. Here we describe a *Pichia pastoris* expression system for GO and compare the kinetic and spectroscopic properties and the 3D structure of Pichia-expressed GO with that from *A. nidulans*. We use this Pichia system to express active-site-mutant proteins and to investigate the roles of Phe464 and Arg330 in substrate binding. We demonstrate that the Arg330-modified proteins are better fructose oxidases than is wild-type GO.

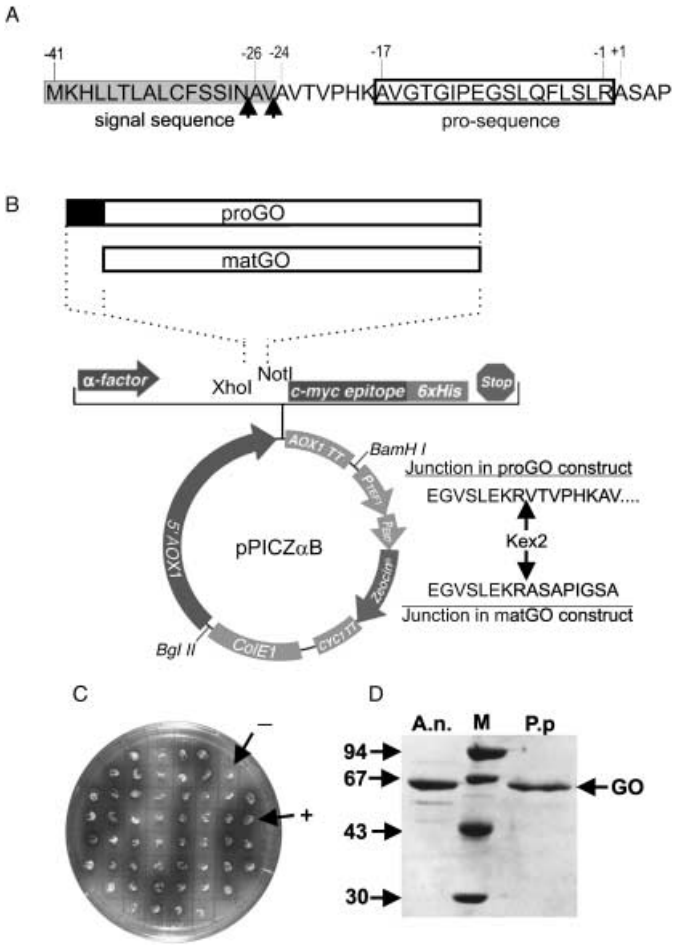


***Figure 2.*** *Galactose oxidase expression in* Pichia pastoris. *A) Annotated sequence of the* N*-terminal region of the precursor GO protein. The predicted signal-sequence cleavage sites are indicated with arrow heads. The pro-region (−17 to −1) identified by* N*-terminal sequencing of the copper-free protein is boxed and the start of the mature protein defined by* N*-terminal sequencing starts at position +1. B) Restriction map of pPICZαB (Invitrogen) with the insert regions introduced to create the proGO and matGO constructs. The resulting junction sequences with the Kex2 cleavage sites are shown. C) Assay plate for selection of GO-expressing clones (+; dark areas) rather than nonexpressors (−; light areas). D) SDS-PAGE showing GO expressed by* Aspergillus nudulans *(A.n.) and GO expressed by* Pichia pastoris *(P.p.). Molecular-mass markers (M) are shown in kDa.*

## Results

### Galactose oxidase expression constructs

The pPICαZ vectors (Figure 2) provide the powerful *AOX1* promoter and the α-mating-factor signal sequence to direct secretion of a fused protein, such as GO, which is naturally secreted by *Fusarium graminearum*. Two similar constructs were generated by using a PCR-based cloning strategy. *N*-terminal signal-sequence prediction was performed by using the SignalP algorithm.[21] The most likely cleavage site is predicted to be between Ala(−26)/Val(−25) with an alternate site at Ala(−24)/Val(−23) (Figure 2A). pPICαZproGO includes the coding sequence from Val(−23) to Arg(−1) at the N terminus of the mature-protein coding region, while pPICαZmatGO contains only the mature-protein coding region starting at Ala(+1) (Figure 2A and B). In both cases the upstream PCR primers were designed to introduce a *Xho*I restriction site to allow in-frame insertion with the upstream α-mating-factor signal sequence of the vector and introduction of a Kex2-like cleavage sequence immediately upstream of the desired *N*-terminal codon, Val(−23) for pPICαZproGO or Ala(+1) for pPICαZmatGO. The same downstream PCR primer was used for both constructs to introduce an additional TGA translation-termination codon and a *Not*I restriction site for cloning into the pPICαZ vector (Figure 2B).

### Screening transformants and liquid culture

A plate-based coupled assay screen for GO activity was used and around 80% of transformants showed enzyme activity

  

(Figure 2C). KM71 clones appeared to display the highest levels of GO activity and were used in further studies.GO was purified from the culture medium by cellulose phosphate chromatography and was then copper-loaded by dialysis.[3] Under these shaken-flask conditions the yields of protein were around 40–50 mg $L^{-1}$ and are therefore comparable with yields achieved from *A. nidulans*.[3] Protein samples were analysed by SDS-PAGE and western blot analysis to determine the level of protein expression and to confirm the identity of the expressed protein as GO. SDS-PAGE revealed a single band migrating at a position corresponding to a 65-kDa protein, as expected for fully processed GO (Figure 2D). Although GO is a 68-kDa protein, the active-site thioether bond leads to conformational constraint in the polypeptide chain and anomalous migration at an apparent molecular mass of 65 kDa.[14]

### *N*-terminal sequencing and mass spectrometry

The *N*-terminal amino acid sequences of the isolated proteins were determined. For pPICαZmatGO, a single sequence with the *N*-terminal sequence ASAPIG was obtained. Electrospray mass spectrometry (ES-MS) indicated a molecular mass of 68513 Da, which corresponds to a protein starting at the expected *N* terminus of the mature protein (predicted $M_r$ = 68516). By contrast the protein produced by the pPICαZproGO construct revealed the presence of multiple species. The predominant *N*-terminal sequence was ASAPIG, comprising >80% of the signal, however, overlapping sequence data, particularly RASAPIG and SLRASAPIG were also identified. ES-MS data confirmed the presence of multiple species with the predominant one corresponding with correctly processed mature GO (68530 Da), but with larger species of 68686 Da (mature protein+Arg; +156 Da; predicted $M_r$ = 68676) and 68887 Da (mature protein+Ser, Leu, Arg; +356 Da; predicted $M_r$ = 68876) also evident. This would be consistent with some level of sequential proteolytic removal of the pro-region. This suggests that in *P. pastoris* the processing of the 17 amino acid pro-sequence may occur by a mechanism distinct from that of filamentous fungi, at least for a proportion of GO molecules.

### X-ray crystal structure

MatGO expressed from pPICZαmatGO was treated with sodium diethyldithiocarbamate to remove the copper, the protein was crystallized and the data processed, scaled and merged with the HKL suite (Table 1). The space group and cell dimensions indicated that the crystals were essentially isomorphous with the original monoclinic wild-type GO crystals. The structure was refined by using the program to a resolution of 1.9 Å, by using initial phases from the Aspergillus-expressed mature structure (PDB code 1GOG). After refinement, the structure of matGO was aligned with the Aspergillus-expressed enzyme (PDB 1GOG) by using the LSQMAN software; this resulted in a RMSD of 0.37 Å which indicates that the two structures are essentially identical with the exception of the copper atom (Figure 3). The structural coordinates have been deposited with the Protein Data Bank under accession code 1T2X.

***Table 1.*** *Data collection and processing statistics for matGO purifed from* P. pastoris. *Figure in brackets indicate values for the highest resolution shell.*

| Data collection statistics | |
|---|---|
| space group | C2 |
| cell dimensions [Å] | $a$ = 96.95, $b$ = 88.52, $c$ = 85.35, $\beta$ = 117.24 |
| resolution range [Å] | 38.3–1.84 |
| no. of observed reflections | 142839 |
| no. of unique reflections | 53734 |
| $I/\sigma[I]$ | 12.8 (3.1) |
| completeness | 96.6 (85.5) |
| $R_{sym}$[a] | 0.039 (0.146) |
| multiplicity | 2.7 |
| **Refinement statistics** | |
| refinement resolution | 30–1.9 |
| $R_{cryst}$[b] | 19.3 |
| $R_{free}$[c] | 21.5 |
| no. of atoms | 5273 |
| RMSD bonds [Å][d] | 0.005 |
| RMSD angles [°][d] | 1.43 |
| RMSD B values (main-chain atoms) [Å][d] | 17.3 |
| RMSD B values (side-chain atoms) [Å][d] | 18.2 |

[a] $R_{sym} = \Sigma_{hkl}(\Sigma_i(|I_{hkl,i} - \langle I_{hkl}\rangle|))/\Sigma_{hkl,i}I_{hkl,i}$, where $I_{hkl,i}$ is the intensity of an individual reflection and $\langle I_{hkl}\rangle$ is the mean intensity of that reflection. [b] $R_{cryst} = \Sigma_{hkl}(||Fobs_{hkl}| - |Fcalc_{hkl}||)/|Fobs_{hkl}|$, where $|Fobs_{hkl}|$ and $|Fcalc_{hkl}|$ are the observed and calculated structure factor amplitudes for reflections used during refinement (working set). [c] $R_{free}$ is equivalent to $R_{cryst}$ but calculated with reflections omitted from the refinement process (test set). [d] RMSD = root mean square deviation.

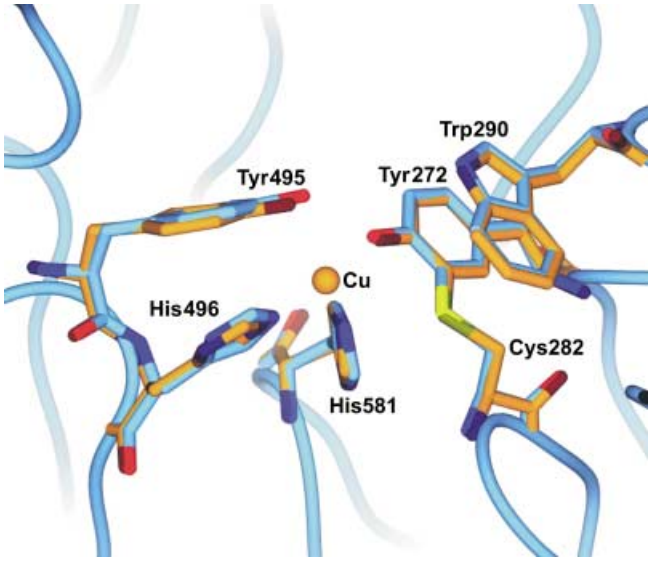


***Figure 3.*** *Superposition of the active site of copper-depleted matGO isolated from* Pichia pastoris *(carbon atoms are pale blue) and the original mature GO structure (PDB code 1GOG; carbon atoms are dark yellow). Copper (yellow sphere) is only present in the original structure as it was removed from matGO by treatment with sodium diethyldithiocarbamate. Otherwise, the structures are essentially identical.*

### UV/Vis spectroscopy

GO is isolated predominantly in a semireduced state ($Cu^{II}$–Y) that can be oxidised to the radical form ($Cu^{II}$–$Y^{-}$) by treatment with the inorganic oxidant ferricyanide or reduced to the inac-

  

tive form ($Cu^{I}$–Y) by ferrocyanide. The UV/Vis spectra of proGO and matGO isolated from *P. pastoris* were essentially identical to those for the enzyme isolated from *A. nidulans*, a result indicating that the active-site environments are identical (data not shown).

### Purification and characterisation of mutational variants

These studies demonstrate that Pichia-expressed matGO is essentially identical to the Aspergillus-expressed enzyme with respect to molecular mass, UV/Vis spectroscopy and 3D structure. We have, therefore, used pPICZαmatGO for the construction and expression of mutational variants to explore the substrate binding and substrate selectivity of GO. The mutational variants, R330K, R330A and F464A, were generated by PCR mutagenesis and the DNA sequence of each mutant gene was confirmed. After protein expression in *P. pastoris* KM71, each protein was purified and copper loaded;[3] the proteins were judged to be greater than 95% pure by SDS-PAGE (Figure 2D). The molecular masses of the variant proteins were determined by ES-MS and are in excellent agreement with the expected masses (data not shown).

### Activity of galactose oxidase and variants with D-galactose

Initial rates of activity were recorded over a substrate range of 10 mM to 1.58 M D-galactose for wild-type GO isolated from *A. nidulans*, matGO and the variants expressed from *P. pastoris*. Values were fitted to the Michaelis–Menton equation by linear regression by using the program Microcal Origin 4.10 and the data are shown in Table 2.

***Table 2.*** *Kinetic parameters for wild-type (WT) GO and mutational variants with D-galactose as the substrate. Catalytic efficiencies (%) relative to the value for WT-matGO (100%) are also shown.*

| | $K_M$ [mM] | $k_{cat}$ [$s^{-1}$] | $k_{cat}/K_M$ [$M^{-1}s^{-1}$] | Relative catalytic efficiency [%] |
|---|---|---|---|---|
| WT-GO from *A. nidulans* | 71.7 ± 7.7 | 855 ± 25 | 11 900 ± 1320 | 114 |
| WT-matGO | 102 ± 6.4 | 1 059 ± 18.9 | 10 400 ± 680 | 100 |
| WT-proGO | 68 ± 5 | 1 090 ± 40 | 16 000 ± 1300 | 154 |
| F464A | 937 ± 124 | 57 ± 4 | 61 ± 9 | 0.6 |
| R330A | 2 240 ± 328 | 84 ± 8.5 | 37 ± 7 | 0.4 |
| R330K | 895 ± 85.9 | 208 ± 10.8 | 232 ± 25 | 2.2 |

The $K_M$ value for the wild-type enzymes shows a modest difference between the enzyme isolated from *A. nidulans* (71.7 mM) and that from *P. pastoris* (102 mM) although there are no other apparent structural or spectroscopic differences between these two enzymes. Variation in the $K_M$ value was also observed by Sun et al.[22] who report a $K_M$ value of 95 mM for native fungal-expressed GO compared with a value of 57 mM for GO expressed in *Escherichia coli*, although this was a variant carrying several mutations that enhance solubility and expression levels. The rate of catalysis, $k_{cat}$, for matGO (1059 $s^{-1}$) is slightly greater than that for GO from *A. nidulans* (855 $s^{-1}$). These differences lead to rather similar values of 10 400 and 11 900 $M^{-1}s^{-1}$, respectively, for the catalytic efficiency of the enzymes.

For the three variants tested, F464A, R330A and R330K, the $K_M$ value for D-galactose was increased substantially, a result indicating less efficient binding of substrate. In addition the catalytic activity of each variant was also substantially reduced, as shown by the lower $k_{cat}$ values. R330A showed the lowest binding affinity for D-galactose with a 22-fold increase in the $K_M$ value (2.2 M) and also showed a 12.6-fold reduction in the $k_{cat}$ value (84 $s^{-1}$). R330K showed an 8.8-fold increase in $K_M$ value (0.9 M) and a more modest reduction of fivefold in the $k_{cat}$ value (208 $s^{-1}$). The F464A mutant showed an increase in the $K_M$ value of about 9.2-fold (0.94 M) but a greater reduction of around 18.6-fold in the $k_{cat}$ value (57 $s^{-1}$). These three variant enzymes are therefore substantially worse than matGO in terms of catalytic efficiency towards D-galactose. R330K is least affected with a $k_{cat}/K_M$ value of 232 $M^{-1}s^{-1}$, some 45-fold lower than matGO. By comparison R330A and F464A show 170- and 250-fold reductions in the $k_{cat}/K_M$ values, to 37 $M^{-1}s^{-1}$ and 61 $M^{-1}s^{-1}$, respectively.

### Activity against a "nonspecific" substrate

The specific activity of the GO mutational variants against the "nonspecific" substrate 3-methoxybenzylalcohol (3MBA) was determined by a direct assay for the aldehyde product. Due to the low miscibility of 3MBA in aqueous buffered solution, it was not possible to determine the $K_M$ and $k_{cat}$ values. Addition of dimethylsulfoxide (DMSO; 10%) allowed a concentration of 3MBA (≈180 mM) to be obtained. The effect on the enzyme of adding DMSO was investigated in the standard 2,2′-azinobis(3-ethylbenzthiazoline-6-sulfonic acid)/horseradish peroxidase (ABTS-HRP) coupled assay; the addition did not adversely affect activity.

The specific activity with matGO (240 mmol $min^{-1}mg^{-1}$) is fourfold lower than with D-galactose. There is a small reduction of around 1.5-fold in the activity of the F464A variant (158 mmol $min^{-1}mg^{-1}$) but a major reduction (63-fold) in the activity of R330K (3.8 mmol $min^{-1}mg^{-1}$). By contrast R330A shows an increase in activity of around 1.4-fold (342 mmol $min^{-1}mg^{-1}$). The difference in activity between the two R330 variants is interesting and presumably reflects a difference in the ability of 3MBA to bind within the active sites of the R330 variants.

### Altered substrate specificity

The alteration of substrate specificity is important for many potential applications of enzymes and we have investigated whether the GO variants affect the oxidation of the alternative substrates D-glucose and D-fructose. Activity against D-glucose was extremely low and so we focussed our studies upon D-fructose, for which the results are shown in Table 3. It was not always possible to directly measure the $K_M$ values for D-fruc-

  

*Table 3. Kinetic parameters for wild-type and mutational variant forms of GO with D-fructose as the substrate.*

| | $K_M$ [M] | $k_{cat}$ [$s^{-1}$] | $k_{cat}/K_M$ [$M^{-1}s^{-1}$] |
|---|---|---|---|
| matGO | 2.48 ± 0.512 | 22.8 ± 3.57 | 9.2 ± 2.4 |
| F464A | 1.85 ± 0.371 | 0.6 ± 0.083 | 0.32 ± 0.8 |
| R330A | 1.81 ± 0.196 | 30.3 ± 2.31 | 16.7 ± 2.2 |
| R330K | 1.07 ± 0.111 | 80.4 ± 5.01 | 75.1 ± 9.1 |

tose due to limitations in the solubility the sugar at high concentrations.

For matGO, the $K_M$ value for D-fructose is projected to be very high (2.48 M) compared with that for D-galactose (102 mM) and the $k_{cat}$ value is also substantially lower (22.8 $s^{-1}$) than the value of 1059 $s^{-1}$ for D-galactose. These effects substantially alter the $k_{cat}/K_M$ ratio, which is reduced from 10400 to 9.2 $M^{-1}s^{-1}$ for D-galactose and D-fructose, respectively. The enzyme is therefore poor at D-fructose oxidation.

The F464A variant also has a higher projected $K_M$ value for D-fructose (1.85 M) than for D-galactose (937 mM) and the $k_{cat}$ value of this variant is also extremely low; at 0.6 $s^{-1}$, it is some 38-fold lower than the $k_{cat}$ value of matGO against D-fructose. This results in a catalytic efficiency ($k_{cat}/K_M$) of only 0.3 $M^{-1}s^{-1}$ for D-fructose, compared with 70 $M^{-1}s^{-1}$ for D-galactose.

The R330A variant also has a high projected $K_M$ value for D-fructose (1.81 mM) but displays a higher $k_{cat}$ value than matGO and therefore an enhanced catalytic efficiency of 16.7 $M^{-1}s^{-1}$, compared with matGO at 9.2 $M^{-1}s^{-1}$. The most active enzyme is R330K, which displays the lowest $K_M$ value (1.07 mM) and highest $k_{cat}$ value (80.4 $s^{-1}$) for D-fructose. The values lead to a catalytic efficiency of 75.1 $M^{-1}s^{-1}$ which is much enhanced over the wild-type enzyme (9.2 $M^{-1}s^{-1}$).

## Discussion

*P. pastoris* is a well-established system for expression of a range of heterologous proteins and has been used to express some constructs encoding GO.[23] We have generated two constructs in which the native secretion signal sequence was replaced by a well-established yeast secretion signal sequence from the α-mating-factor protein. Both constructs led to production of similar amounts of protein in shaken-flask cultures. The matGO protein has a single *N*-terminal sequence consistent with efficient Kex2-like-mediated removal of the signal sequence to reveal the mature N terminus. This observation is in agreement with the results of Whittaker and Whittaker,[23] who used a glucoamylase signal sequence to express mature GO. ES-MS analysis, UV/Vis spectroscopy and 3D structure determination indicate that matGO produced in *P. pastoris* is essentially identical to Aspergillus-expressed GO.

We have used this expression system to examine the properties of mutational variants. A molecular model for substrate binding is supported by recent evidence from a study by Sun et al.[20] focussing on Trp290, Arg330 and Gln406 and from our own studies on the W290F variant (M. Rogers, K.M., P.F.K., S.E.V.P., M.J.M. and D. M. Dooley, unpublished data).

We have now shown the importance of Phe464, one of two phenylalanine residues that provide a hydrophobic surface that lines one side of the active site. Loss of the phenyl ring in F464A leads to a 9.2-fold increase in the $K_M$ value, an approximately 18.6-fold reduction in the $k_{cat}$ value and, thus, a 170-fold reduction in catalytic efficiency. This may arise as a result of the increased space available within the active site leading to suboptimal binding of the substrate for catalysis. When the nonspecific substrate 3MBA is used, there is a less pronounced effect of this mutation since 3MBA is a somewhat poorer substrate for matGO.

For Arg330, proposed from model studies[12,13,17] to interact with the O(3) and O(4) atoms of D-galactose, we made two alterations, R330A to remove the large guanidinium side chain and thus prevent any possible hydrogen bonding to the substrate and R330K to provide a side chain potentially capable of forming a single hyrogen bond. Modelling studies, however, reveal that the Arg330 side chain is extended in order to hydrogen bond with D-galactose and that a Lys side chain in this position is too far from D-galactose to make a hydrogen-bond interaction without some repositioning of the substrate or movement of the Cα backbone. Wachter and Brandchaud[17] suggest that R330 may help to stabilise the transition state.

In R330A the $K_M$ value is affected most substantially, increasing to a projected 2.2 M, a 22-fold increase, while the $k_{cat}$ value is reduced to 84 $s^{-1}$; R330A is therefore the least efficient variant with D-galactose, a fact demonstrating that the guanidinium side chain of Arg330 is important in substrate binding. When a substrate such as 3MBA, which is incapable of forming such hydrogen bonds, is used, R330A proves to be even more effective than matGO.

Despite the evidence that the lysine side chain in R330K would not allow formation of a hydrogen bond to D-galactose, the kinetic parameters for this variant are better than those for R330A. The $K_M$ value (895 mM) is still higher than for matGO (102 mM) but the $k_{cat}$ value (208 $s^{-1}$) is some fivefold lower, results leading to a 45-fold reduction in catalytic efficiency. It is possible there is some rearrangement of either the substrate or the enzyme main chain within the active site to allow formation of a hydrogen-bond interaction between Lys330 and D-galactose or with the transition state. It is unclear why the presence of the lysine side chain leads to a substantial reduction in efficiency for oxidation of 3MBA relative to the wild-type enzyme (63-fold) and the R330A variant (90-fold) that lacks the long side chain.

A major goal of enzyme engineering is the redesign of existing enzymes to catalyse reactions with new substrates. Sun et al.[20] have reported the acquisition of a low level of glucose oxidase activity following a saturation mutagenesis study of the residues Arg330, Trp290 and Gln406. Another important substrate for which enhanced oxidase activity would be useful is D-fructose. This sugar is widely used in the food industry but represents a poor substrate for wild-type GO. Alternative D-fructose assay systems rely on either D-fructose dehydrogenase systems, which tend to be complex, multisubunit enzymes, some of which are membrane bound or have dissociable cofactors such as pyrroloquinoline quinone, or on multienzyme

  

reactions that are often used to measure both glucose and fructose. A GO-derived fructose oxidase is an attractive proposition since the enzyme is monomeric and soluble and it requires only copper to be added to generate its own intrinsic organic cofactor and support catalysis.

MatGO has a $K_M$ value for D-fructose higher than the $K_M$ value for D-galactose (2.5 and 0.1 M, respectively) while the $k_{cat}$ value is substantially lower (23 and 1059 $s^{-1}$, respectively). MatGO therefore displays a much lower $k_{cat}/K_M$ ratio for D-fructose (9.2 $M^{-1}$ $s^{-1}$) than for D-galactose (10400 $M^{-1}$ $s^{-1}$), a fact supporting the observation that the enzyme is a poor D-fructose oxidase.

By contrast, the R330 variants display a shift in favour of D-fructose as the substrate. The best variant is R330K, where the $K_M$ value is more favourable (1.07 M) and the $k_{cat}$ value is higher (80.4 $s^{-1}$). This leads to an 8.2-fold increase in the $k_{cat}/K_M$ ratio for R330K with D-fructose compared with that for matGO with the same substrate (Table 3). Comparing the efficiency constant values ($k_{cat}/K_M$) provides a measure of substrate selectivity between D-fructose and D-galactose. For matGO these values are 9.2 and 10400 $M^{-1}$ $s^{-1}$, respectively, and for R330K they are 75.1 and 232 $M^{-1}$ $s^{-1}$, respectively. Table 4 provides a comparison of the relative activities of the enzymes and the level of discrimination they display against the two substrates. It is clear that matGO shows a high level of discrimination (1130-fold) in favour of D-galactose. By comparison R330K shows much less discrimination (only threefold) in favour of D-galactose. While R330K is rather a poor enzyme against D-fructose, it is a significantly better fructose oxidase than the wild-type matGO. Studies to investigate the effects of R330 variants in combination with other mutations within the active site of GO are underway in an attempt to enhance further the fructose oxidase activity of GO.

***Table 4.*** *Comparisons of percentage values for $k_{cat}/K_m$ for D-galactose and D-fructose as substrates. Values are shown relative to 100% for matGO. Comparison of the values for the two substrates provides an indicator of the discrimination that each enzyme possesses for the two substrates and emphasises the reduced discrimination in the R330 variants. No discrimination would result in a value of 1. The more positive the value the greater the selectivity for D-galactose over D-fructose.*

| | Percent wild-type activity against D-galactose | Percent wild-type activity against D-fructose | Fold-difference in preference for D-galactose over D-fructose |
|---|---|---|---|
| matGO | 100 | 100 | 1130 |
| F464A | 0.6 | 3.3 | 203 |
| R330A | 0.4 | 182 | 2.21 |
| R330K | 2.2 | 816 | 3.1 |

## Experimental Section

**Construct generation and *P. pastoris* transformation**: The Easy Select *P. pastoris* expression system from Invitrogen was used as a source of expression vectors and strains. The *N*-terminal amino acid sequence of the GO-encoding gene is shown in Figure 2A. GO is produced initially with an *N*-terminal leader sequence including a secretion signal sequence that is removed during passage into the endoplasmic reticulum. The remaining portion of the leader sequence, termed the pro-region, is then removed, the cofactor thioether bond forms and the radical is generated to give matGO, the active enzyme. Two constructs were generated, both exploiting the α-mating-factor secretion signal sequence present in the pPICZαB vector (Figure 2B). The appropriate DNA fragments were amplified from pGOF102[3] by PCR with the forward primers A (for proGO) and B (for matGO), together with the reverse primer C.

A: 5′-TGCTTCAGCAAGCTT**CTCGAG**AAAAGAGTCACCGTCCCTCACAAGGCCG-3′

B: 5′-GGGAGTCTTAAGCTT**CTCGAG**AAAAGAGCCTCAGCACCTATCGGAAGCGCC-3′

C: 5′-TCCTATGAAAAAGCTT**GCGGCCGC**TCATCACTGAGTAACGCGAATCGTCGAAGC-3′

Restriction sites (bold) introduced by the primers were *Xho*I in primers A and B and *Not*I in primer C to facilitate subsequent cloning of the amplified fragments. Each reaction contained pGOF102 DNA (1 ng), each primer (50 pmol) and each deoxynucleoside triphosphate (dNTP; 200 nM). Reactions were performed in a Hybaid OmniGene thermal cycler and the proofreading DNA polymerase *Pwo* (Boehringer Mannheim) was added following the initial template denaturation step (95 °C, 2 min) to ensure hot start conditions. Thermal cycling for 30 cycles of 95 °C for 30 s, 55 °C for 1 min and 72 °C for 2 min, with a final step of 72 °C for 5 min, was performed. The PCR products were digested with *Xho*I and *Not*I, purified by recovery from an agarose gel and then ligated[24] with *Xho*I/*Not*I-digested pPICZαB vector DNA. After transformation into *E. coli* TOP10 cells (Invitrogen), transformants were selected on AMBA agar plates[24] containing Zeocin (25 μg $mL^{-1}$; Invitrogen) and were screened for the presence of recombinant plasmids by using a Quantum Prep kit (Bio-Rad). Restriction digestion with *Xho*I and *Not*I was used to confirm the presence of inserts of the expected size. Representative plasmids, termed pPICαproGO and pPICαmatGO, were selected and the inserted fragments were confirmed by DNA sequence analysis.

DNA for the transformation of *P. pastoris* was linearized within the *AOX1* promoter region by *Sac*I digestion and then purified from an agarose gel. Linearised DNA (10 μg) was gently mixed with electrocompetent cells (80 μL) and electroporated in a 0.2-cm cuvette at 200 Ω resistance, 25 μF capacitance and 1500 V charge potential. Immediately, ice-cold sorbitol (1 mL, 1 M) was added and the cells were allowed to recover for two hours at 30 °C, before being plated onto yeast extract peptone dextrose (Invitrogen manual) plates containing zeocin (100 μg $mL^{-1}$). *P. pastoris* strains KM71 (*AOX1*Δ*:SARG4,His4,Arg4*), GS115 (*His4*) and X-33 were transformed.

**Plate assay for GO-expressing transformants**: Transformants were streaked onto minimal medium agar plates containing methanol (0.5%) and a GO assay mixture of D-galactose (2%), ABTS (1.2 mg $mL^{-1}$) and HRP (0.04 U $mL^{-1}$).[3]. Expression of active GO was revealed by the development of a green colour (Figure 2C).

**Generation, purification and characterisation of mutational variants**: Mutants were generated by a PCR splicing by overlap extension (SOEing) approach.[25] The following primers were used to generate the mutations R330K, R330A and F464A, respectively. For the mutagenic primers the altered codons are in italics and the altered nucleotides are highlighted in bold. The *Xho*I and *Not*I restric-

  

tion sites in the flanking primers, GOf and GOr, respectively, are in bold.

R330K: 5′-TGTAC***AAG***TCAGACAACCACG-3′

R330A: 5′-TGTAC***GCT***TCAGACAACCACG-3′

F464A: 5′-TCCG***GC***CGAGGATTCAACCCCG-3′

GOf: 5′-GGGAGTCTTAAGCTT**CTCGAG**AAAAGAGCCTCAGCACCT-ATCGGAAGCGCC-3′

GOr: 5′-TCCTATGAAAAAGCTT**GCGGCCGC**TCATCACTGAGTAACG-CGAATCGTCGAAGC-3′

A two-stage PCR was performed. The first PCR comprised pGOF102 template DNA (50 ng),[3] the appropriate mutagenic primer (50 pmol) and GOr (50 pmol) in *Taq* buffer containing each dNTP (200 μM) and *Taq* DNA polymerase (1 U) and was subjected to the following temperature cycling in an MJR PCT100 instrument: 95 °C for 5 min then 35 cycles of (95 °C for 1 min, 55 °C for 1 min and 72 °C for 1 min) then 72 °C for 5 min. This generated a PCR fragment that was purified from an agarose gel. An aliquot of this DNA (10 pmol) was used as a megaprimer in the second PCR, together with primer GOf (25 pmol), pGOF102 template DNA (5O ng), *Taq* reaction buffer, each dNTP (200 μM) and *Taq* DNA polymerase (0.5 units) with the following temperature cycling: 95 °C for 5 min then 20 cycles of (95 °C for 1 min, 55 °C for 1 min and 72 °C for 2 min) then 72 °C for 5 min. The final product was digested with *Xho*I and *Not*I, purified from an agarose gel, and cloned into the *Xho*I- and *Not*I-digested pPICZαB vector. Mutant clones were confirmed by DNA sequence analysis and the clones were designated pPICαZmatGO:R330A, pPICαZmatGO:R330K and pPICαZematGO:F464A. Aliquots of each plasmid (2 μg) were digested with *Sac*I and transformed into electrocompetent *P. pastoris* KM71 as described above.

**Protein purification and analysis**: For medium-scale protein purification, cultures (1–2 L) were grown to an optical density at 600 nm of 2–6 then cells were harvested by centrifugation at 3000 *g* for 5 min, resuspended in buffered complex methanol medium (Invitrogen Easyselect manual) containing copper sulfate (0.5 mM) and methanol (0.5 % *v/v*), to induce expression of GO, and grown for a further 48 h at 25 °C. A further addition of methanol (0.5 % *v/v*) was made after 24 h.[23] Samples of supernatant were analysed by SDS-PAGE and a western blot with a rat anti-GO antiserum as the primary antibody and a peroxidase-conjugated anti-rat IgG as the secondary antibody,[3] with ECL chemiluminescent detection (Amersham Pharmacia Biotech) according to the manufacturers' protocol. Protein was purified essentially according to the method of Baron et al.[3] Briefly this involved ammonium sulfate precipitation (30–80 % fraction) with the pellet redissolved in sodium phosphate buffer (10 mM, pH 7.3) and dialysed against the same buffer (300 volumes). The sample was loaded onto a cellulose phosphate column equilibrated in the same buffer and GO was eluted by applying a gradient of sodium phosphate (10–100 mM, pH 7.3). GO-containing fractions were concentrated by using an Amicon ultrafiltration cell. The protein was then copper loaded by dialysis[3] and samples were analysed by SDS-PAGE. Mutant proteins were purified by using the same procedure. Protein concentrations were determined by measuring the absorbance at 280 nm and using an extinction coefficient of 104 900 $cm^{-1}\,M^{-1}$.[26]

***N*-terminal amino acid sequencing and mass spectrometry**: After electroblotting from SDS-PAGE onto polyvinylidene fluoride (PDVF) membrane and staining with sulforhodamine B (Sigma), protein bands were submitted for *N*-terminal amino acid sequence analysis in the Biomolecular Analysis Facility at the University of Leeds. For mass spectrometry, samples were prepared by diluting in sterile deionised water to a concentration of 20–50 pmol $\mu L^{-1}$ and then dialysing for 36 h against 3 changes of deionised water (2500 volumes). Samples were treated with formic acid (0.05 %, pH 2.0) prior to analysis with a QTOF mass spectrophotometer (Micromass, UK) to provide molecular mass information.

**UV/Vis spectrophotometry**: Samples (8 mg $mL^{-1}$) were oxidized by incubating with potassium ferricyanide (0.05 M) for 5 min. Oxidant was removed on a P-6DG resin (BioRad) into sodium phosphate buffer (100 mM, pH 7.0). Oxidized GO is green in colour, a fact allowing efficient collection of protein-containing fractions. Spectra were measured in a Shimadzu UV-2401PC spectrophotometer at 25 °C over the range 200–900 nm.

**Galactose oxidase assay and kinetic analysis**: For specific activity measurements, a coupled assay system, based on the method of Amaral et al.,[27] was used. The assay reagent mixture (20 mL) contained D-galactose (2.16 g), ABTS (11 mg) and HRP (300 U) in sodium phosphate buffer (100 mM, pH 7.0). An aliquot of protein solution (50 μL) was mixed with the assay reagent (0.95 mL) and the rate of change in absorbance was measured at 405 nm and 25 °C. Two molecules of ABTS are oxidized for each molecule of $H_2O_2$ generated by GO and an extinction coefficient for the ABTS cation radical of 29 300 $cm^{-1}\,M^{-1}$ at 405 nm was used to calculate enzyme activity.

Enzyme kinetic measurements were performed by using this assay system and varying the concentration of substrate from 10 mM to 1.58 M for D-galactose and from 47.5 mM to 1.52 M for D-fructose. The $K_M$ and maximum rate of catalysis, $V_{max}$, values were calculated by using a curve-fitting function in the Origin 4.1 program (MicroCal) to fit the data to the Michaelis–Menten equation. Enzyme assays with 3-methoxybenzylalcohol were made by a direct assay to detect the product aldehyde, which displays an absorption maximum at 314 nm. The low solubility of this "nonspecific" substrate prevented determination of kinetic parameters.

**Crystallization and structure determination**: As part of our studies on the processing of GO and the role of copper in the active site, matGO expressed from pPICZαmatGO was treated with a tenfold excess of sodium diethyldithiocarbamate to remove the copper. It was crystallised in PEG 8000 (16 %), β-morpholinoethanesulfonic acid (200 mM) and calcium acetate (100 mM) by using the sitting-drop method at 18 °C. Rod-shaped crystals of 40×60×300 μm grew within 2 weeks. A data set was collected by Dr J. Jaeger at DESY synchrotron, Hamburg, on station X11 at a wavelength of 1.28 Å, by using a MAR 345 detector.

## Acknowledgements

*We thank Christian Kurtis for assistance in producing Figure 1 and Jo Jaeger for crystallographic data collection. We also thank Alison Ashcroft for mass spectrometry and guidance in data analysis, Denise Ashworth for DNA sequence analysis and Jeff Keen for* N*-terminal sequence analysis, all within the Biomolecular Analysis Facility in Leeds. We are grateful to Alfred Haandrikman and Astrid Mars for helpful discussions. Financial support from Hercules Incorporated and the Biotechnology and Biological Sciences Research Council (BBSRC) are gratefully acknowledged. K.M. was in receipt of an Egyptian Government Studentship and S.J.F. was funded by a BBSRC studentship.*

  

**Keywords:** copper enzymes · enzyme catalysis · fructose · oxidases · protein engineering

[1] Z. B. Ogel, D. Brayford, M. J. McPherson, *Mycol. Res.* **1994**, *98*, 474.
[2] M. L. Niessen, R. F. Vogel, *Syst. Appl. Microbiol.* **1997**, *20*, 111.
[3] A. J. Baron, C. Stevens, C. Wilmot, K. D. Seneviratne, V. Blakeley, D. M. Dooley, S. E. Phillips, P. F. Knowles, M. J. McPherson, *J. Biol. Chem.* **1994**, *269*, 25095.
[4] M. S. Rogers, A. J. Baron, M. J. McPherson, P. F. Knowles, D. M. Dooley, *J. Am. Chem. Soc.* **2000**, *122*, 990.
[5] S. J. Firbank, M. S. Rogers, C. M. Wilmot, D. M. Dooley, M. A. Halcrow, P. F. Knowles, M. J. McPherson, S. E. V. Phillips, *Proc. Natl. Acad. Sci. USA* **2001**, *98*, 12932.
[6] G. T. Babcock, M. K. Eldeeb, P. O. Sandusky, M. M. Whittaker, J. W. Whittaker, *J. Am. Chem. Soc.* **1992**, *114*, 3727.
[7] M. M. Whittaker, J. W. Whittaker, *Abstr. Pap. Am. Chem. Soc.* **1988**, *195*, 553.
[8] M. M. Whittaker, V. L. DeVito, S. A. Asher, J. W. Whittaker, *J. Biol. Chem.* **1989**, *264*, 7104.
[9] M. M. Whittaker, J. W. Whittaker, *J. Biol. Chem.* **1990**, *265*, 9610.
[10] M. L. McGlashen, D. D. Eads, T. G. Spiro, J. W. Whittaker, *J. Phys. Chem.* **1995**, *99*, 4918.
[11] J. W. Whittaker, *Methods Enzymol.* **1995**, *258*, 262.
[12] N. Ito, S. E. Phillips, C. Stevens, Z. B. Ogel, M. J. McPherson, J. N. Keen, K. D. Yadav, P. F. Knowles, *Nature* **1991**, *350*, 87.
[13] N. Ito, S. E. V. Phillips, K. D. S. Yadav, P. F. Knowles, *J. Mol. Biol.* **1994**, *238*, 794.
[14] M. J. McPherson, C. Stevens, A. J. Baron, Z. B. Ogel, K. Seneviratne, C. Wilmot, N. Ito, I. Brocklebank, S. E. V. Phillips, P. F. Knowles, *Biochem. Soc. Trans.* **1993**, *21*, 752.
[15] M. P. Reynolds, A. J. Baron, C. M. Wilmot, E. Vinecombe, C. Stevens, S. E. V. Phillips, P. F. Knowles, M. J. McPherson, *J. Biol. Inorg. Chem.* **1997**, *2*, 327.
[16] C. G. Saysell, T. Barna, C. D. Borman, A. J. Baron, M. J. McPherson, A. G. Sykes, *J. Biol. Inorg. Chem.* **1997**, *2*, 702.
[17] R. M. Wachter, B. P. Branchaud, *J. Am. Chem. Soc.* **1996**, *118*, 2782.
[18] A. Maradufu, A. S. Perlin, *Carbohydr. Res.* **1974**, *32*, 93.
[19] G. Avigad, D. Amaral, C. Asensio, B. L. Horecker, *J. Biol. Chem.* **1962**, *237*, 2736.
[20] L. H. Sun, T. Bulter, M. Alcalde, I. P. Petrounia, F. H. Arnold, *ChemBioChem* **2002**, *3*, 781.
[21] H. Nielsen, J. Engelbrecht, S. Brunak, G. von Heijne, *Protein Eng.* **1997**, *10*, 1.
[22] L. H. Sun, I. P. Petrounia, M. Yagasaki, G. Bandara, F. H. Arnold, *Protein Eng.* **2001**, *14*, 699.
[23] M. M. Whittaker, J. W. Whittaker, *Protein Expression Purif.* **2000**, *20*, 105.
[24] J. Sambrook, E. F. Fritsch, T. Maniatis, *Molecular Cloning*, 2nd ed., Cold Spring Harbor Laboratory Press, Cold Spring Harbor, **1989**.
[25] G. Sarkar, S. S. Sommer, *Biotechniques* **1990**, *8*, 404.
[26] D. J. Kosman, M. J. Ettinger, R. E. Weiner, E. J. Massaro, *Arch. Biochem. Biophys.* **1974**, *165*, 456.
[27] D. Amaral, L. Bernstein, D. Morse, B. L. Horecker, *J. Biol. Chem.* **1963**, *238*, 2281.

Received: October 30, 2003

  